Reconfigurable Intelligent Surface Placement in 5G NR/6G: Optimization and Performance Analysis

Gianluca Brancati*, Olga Chukhno*,‡, Nadezhda Chukhno*,†, and Giuseppe Araniti*
*University Mediterranea of Reggio Calabria, Italy and CNIT, Italy
†Universitat Jaume I, Castelló de la Plana, Spain
‡Tampere University, Finland
e-mail: *gianluca.brancati97@gmail.com,* {*olga.chukhno, nadezda.chukhno, araniti*}*@unirc.it*

***Abstract*—The reconfigurable intelligent surface (RIS) adoption has drawn significant attention for the upcoming generation of cellular networks, i.e., 5G New Radio (NR)/6G, as a technology for forming virtual line-of-sight (LoS) links during human blockage or non-line-of-sight (NLoS) transmissions. However, the exploration of RIS placement under realistic conditions of multiple user operations has been limited by 1-2 user scenarios, but still is crucial since RIS deployment affects system performance. This paper addresses the challenge of optimal RIS deployment in 5G NR/6G cellular networks with directional antennas. Specifically, we formulate the RIS deployment problem as a facility location problem that maximizes the total data rate. We then evaluate and analyze the impact of various parameters on RIS-aided communications, such as RIS height, blockers density, number of users, and user distribution. The results confirm that the optimal RIS placement is near the BS for the case of uniform and cluster user distributions with RIS height of more than 5 m and close to the hotspots in the case of the cluster user distribution with RIS height of less than 5 m.**

***Index Terms*—5G NR/6G, cellular networks, network planning, mmWave, reconfigurable intelligent surfaces, deployment.**

I. Introduction

New disruptive technologies, such as autonomous driving, extended reality, and other wearable applications, have stringent data rate, reliability, and latency requirements, which cannot be satisfied by the current generation of cellular networks. To this end, network operators, telecommunication enterprises, and universities are elaborating on the new technological innovations, including but not limited to terahertz communications, visible light communications, and non-terrestrial networks, to enhance network performance [1]. Another and one of the most exciting breakthroughs is forecasted to be reconfigurable intelligent surface (RIS), often referred to as intelligent reconfigurable surface (IRS), large intelligent surface (LIS), or digitally controllable scatterers.

A RIS is a planar surface composed of numerous low-cost reflective elements, each of which can independently shape the amplitude and phase shift of an impinging signal [2]. RISs are expected to overcome limitations of directional systems in the case of human blockage or non-line-of-sight (NLoS) situations and become game-changers in future 5G New Radio (NR)/6G cellular network developments thanks to their flexibility, environment friendliness, compatibility with other telecommunication technologies, and ability to manipulate radio environment behavior. Despite these advantages, there are still many open questions and challenges regarding RIS development and employment. RIS deployment is but one of the problems to tackle more urgently since it affects system performance.

Some recent studies have focused on the RIS deployment positions considering $1-2$ users only. Specifically, in [3], a single RIS deployment in a network with one user and one base station (BS) has been analyzed. According to [3], the received signal-to-noise ratio (SNR) is maximized when a RIS is placed either near the user or the BS. In [4] and [5], the capacity region of a communication network with two users, an access point, and M RIS reflective elements has been investigated. Regarding the RIS configuration, both distributed (where reflective elements are placed on different RISs) and centralized (where all reflective elements are placed on a single RIS) deployment strategies have been studied. Furthermore, according to [4] and [5], the centralized deployment outperforms the distributed one, especially when the users have asymmetric rate requirements and/or channel conditions.

In addition, in [6], the performance of a RIS-aided communication system for centralized and distributed RIS implementations has been analyzed, where RISs are subject to outdated channel state information. The distributed deployment might outperform the centralized one when *(i)* one RIS is placed near the BS, *(ii)* one RIS is placed near the user, and *(iii)* multiple RISs communications are employed. Furthermore, a RIS positioned near the user grants a better ergodic capacity and energy consumption than a RIS deployed near the BS [6]. Differently, in [7], an aerial-RIS system to support ultra-reliable low latency communication (URLLC) and an optimization framework to solve a aerial-RIS deployment and resource allocation problem have been proposed. Finally, in [8], the deployment strategy of a single RIS in a relay-aided wireless system has been studied. According to [8], placing the RIS near the relay maximizes the achievable rate of the system.

In summary, the performance of different RIS deployment configurations has been analyzed in [4]–[6]. Still, a RIS deployment problem has been formalized and solved only in [7] and [8] for aerial-RIS scenario and a relay-aided system, respectively, which are slightly different from classic terrestrial cellular network scenarios. The optimal RIS deployment for a scenario with multiple users has not been sufficiently

This is the post-print of the following article: Brancati, G., Chukhno, O., Chukhno, N., Araniti, G. (2022, September). Reconfigurable Intelligent Surface Placement in 5G NR/6G: Optimization and Performance Analysis. Article has been published in final form at: https://ieeexplore.ieee.org/abstract/document/9978019.
DOI: 10.1109/PIMRC54779.2022.9978019

examined. In this paper, to fill this gap, we formulate a RIS deployment problem as a facility location problem, which allows us to maximize the total data rate of the cellular network, thereby revealing optimal RIS deployment positions. We also analyze the proper RIS height and investigate the impact of different parameters on RIS-aided communications. Our results confirm that the optimal RIS placement is near the BS for uniform and cluster user distribution with RIS height of more than 5 m. For cluster user distribution with RIS height of less than 5 m, the RISs should be near the hotspots.

II. System Model

This section introduces the reference system model. We begin with the deployment, antenna, propagation, and blockage models. Then, we elaborate on propagation under RIS deployment. The representative example of the considered RIS-assisted system is presented in Fig. 1.

A. Deployment, Antenna, Propagation, and Blockage Models

We consider a 5G NR/6G cellular outdoor deployment, where all user equipment (UE) devices are provided with millimeter wave (mmWave) modules and served by an NR BS that operates at the central frequency of 28 GHz waveband. The height of the NR BS is assumed to be constant and set to h_{BS}. The geometric locations of N_{UE} UEs, $\mathcal{N}_{\text{UE}} = \{1, ..., N_{\text{UE}}\}$, are assumed to be uniformly distributed in the plane / according to a Matérn cluster point process with K clusters. We investigate a downlink single unicast session provisioning to N_{UE} UEs.

We assume that devices transmit directionally with an antenna pattern akin to a conical shape, i.e., with a unique beam shape in both elevation and azimuth planes. To this end, for numerical tractability, we approximate the beamforming design as proposed in [9] with the transmit antenna gain:

$$G_{\text{tx}} = D_0 \rho(\alpha), \tag{1}$$

where D_0 is the maximum directivity along the antenna boresight, α is the angular deviation of the transmit/receive direction from the antenna boresight for a receiver, $\rho(\alpha) \in [0; 1]$ is a linear function that scales the directivity D_0 [9] , which, in turn, depends on the number of antenna elements, N_{AE}.

We adopt the 3GPP urban microcell (UMi) Street Canyon path loss model in [10]. We consider UEs in one of the following states: line-of-sight (LoS) non-blocked, LoS blocked, NLoS non-blocked, or NLoS blocked. NLoS state means that buildings can block the path between the BS and the UE, whereas the human blockage attenuation of 15 dB is due to the possible presence of UEs close to the destination with the constant blocker density, λ_B. The UEs' and blockers' heights are constants and given by h_{UE} and h_B, respectively. The blockers are modeled as cylinders with radius r_B.

Then, the associated UMi path loss for a general state measured in dB is given by [11]:

$$L_{dB}(y) = \beta + 10\zeta \log_{10} y + 20 \log_{10} f_c, \tag{2}$$

where f_c is the carrier frequency in GHz, y is the three-dimensional (3D) distance between the BS and the UE, β and ζ are blockage and propagation coefficients, respectively. Note that β and ζ assume different values according to UE conditions, e.g., $\zeta = 2.1$ and $\zeta = 3.19$ in the case of LoS and NLoS conditions, whereas $\beta = 32.4$ and $\beta = 47.4$ if the UE is in non-blocked and blocked states, respectively.

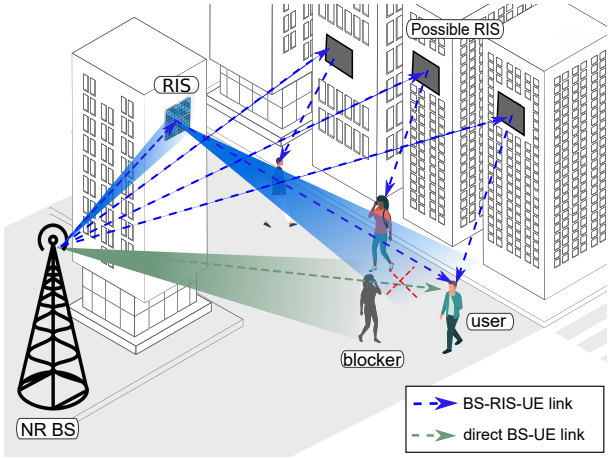

Fig. 1. Illustration of considered RIS-assisted system.

The path loss defined in (2) can be written in the linear scale by utilizing the generic representation $L(y) = Ay^{\zeta}$, where $A = 10^{2 \log_{10} f_c + \beta}$, while the human blockage probability at the 3D distance y is determined as in [12]:

$$p_B(y) = 1 - \exp^{-2\lambda_B r_B \left[\sqrt{y^2 - (h_{\text{BS}} - h_{\text{UE}})^2} \frac{h_B - h_{\text{UE}}}{h_{\text{BS}} - h_{\text{UE}}} + r_B\right]}, \tag{3}$$

where λ_B is the blockers density, h_B and r_B are the blockers' height and radius, and h_{UE} is the UE height, $h_B \geq h_{\text{UE}}$.

We then introduce a building blockage model required while considering city deployments. The LoS probability for the 2D distance x between the BS and the UE, $p_L(x)$, can be obtained by using the 3GPP UMi Street Canyon model [10] as follows:

$$p_L(x) = \begin{cases} 1, & x \leq 18\text{m}, \\ 18 + xe^{-\frac{x}{36}} - 18e^{-\frac{x}{36}}, & x > 18\text{m}. \end{cases} \tag{4}$$

Then, the total received power at distance y is given by

$$P_{\text{rx}} = P_{\text{tx}} G_{\text{tx}} G_{\text{rx}} L^{-1}(y) = \frac{P_{\text{tx}} G_{\text{tx}} G_{\text{rx}}}{L(y)}, \tag{5}$$

where $G_{\text{tx}} = D_0 \rho(\alpha)$ is the transmit antenna gain, G_{rx} is the receive antenna gain, and $L(y)$ is a linear path loss.

B. RIS Propagation Model

Assumption 1 (perfect channel state information) [13]. We assume that the BS knows the perfect channel state information (CSI) for both BS-UE and BS-RIS-UE links.

Assumption 2 (RIS configuration) [14]. The RIS is composed of $M_{SE} \times N_{SE}$ sub-wavelength elements, each with the size of $s_{M_{SE}} \times s_{N_{SE}}$. We assume that $D_{m,n}$ and $d_{m,n}$ are the distances between the BS and the (m, n)-th RIS element and between the (m, n)-th RIS element and the UE, respectively.

Assumption 3 (far-field). We consider far-field propagation, meaning that the distances from different RIS elements to

the BS or a UE are approximately the same, i.e., $D_{m,n} = d_{\text{SR}}$ or $d_{m,n} = d_{\text{RD}}$, where d_{SR} is the distance between the BS (source) and the center of the RIS, whereas d_{RD} is the distance between the center of the RIS and a UE (destination). Hence, the channel gain is the same for all RIS reflecting elements.

Similarly to BS-UE links, 3GPP UMi-Street Canyon model is utilized to express the path loss of sub-paths, which are defined from source, i.e., BS, to RIS, $L(d_{\text{SR}})$, and from RIS to destination, i.e., UEs, $L(d_{\text{RD}})$. The total received power at the UE side through the RIS element i is calculated as in [15]:

$$P_{\text{rx},i} = \frac{P_{\text{tx}}|\Gamma_i|G_{\text{tx}}G_{\text{rx}}}{L(d_{\text{SR}})L(d_{\text{RD}})}, \tag{6}$$

where Γ_i is the reflection coefficient of RIS element i:

$$\Gamma_i = e^{-j\varphi_i} G_i^e G_r^e \epsilon_b, \tag{7}$$

where φ_i is the phase difference induced by RIS element i, G_i^e is the gain of the RIS in the direction of the incoming wave, G_r^e is the gain of RIS in the direction of the received wave, and ϵ_b is the efficiency of RIS, which is described as the ratio of transmit signal power by RIS to received signal power by RIS. In this paper, we assume that $\epsilon_b = 1$.

The total received power at the receiver (including all RIS elements) is expressed as

$$P_{\text{rx},i} = \left(\sum_i \sqrt{\frac{P_{\text{tx}}|\Gamma_i|G_{\text{tx}}G_{\text{rx}}}{L(d_{\text{SR}})L(d_{\text{RD}})}} e^{j\phi_i} \right)^2, \tag{8}$$

where ϕ_i represents the phase delay of the signal received through RIS element i.

Assumption 4 [16]. For simplicity, we assume that RIS-elements reflect signal with unit-gain reflection coefficients ($|\Gamma_i| = 1$) and in a such way that all the signals coming through different RIS elements are aligned in phase at the receiver ($\phi_i = \varphi_i$). Then, (8) becomes

$$P_{\text{rx},i} = \left(\sum_i \sqrt{\frac{P_{\text{tx}}G_{\text{tx}}G_{\text{rx}}}{L(d_{\text{SR}})L(d_{\text{RD}})}} \right)^2. \tag{9}$$

Therefore, the total path loss is given by

$$L_{TOT} = \left(\sum_i \sqrt{\frac{1}{L(d_{\text{SR}})L(d_{\text{RD}})}} \right)^{-2}. \tag{10}$$

The SNR in presence of a RIS can be then derived as

$$\gamma = \frac{P_{\text{tx}}G_{\text{tx}}G_{\text{rx}}}{N_0 W L_{TOT}}, \tag{11}$$

where N_0 is the power spectral density of noise, whereas W is the operating bandwidth in Hz.

The data rate in the presence of a RIS can be calculated according to the Shannon-Hartley theorem:

$$D[\text{Gbps}] = W_{\text{GHz}} \log_2(1+\gamma), \tag{12}$$

where γ is the SNR in linear scale, W_{GHz} is the operating bandwidth in GHz.

III. Optimization Formulation

This section describes the optimization framework for the optimal RIS deployment problem formulated as a facility location problem [17] by targeting the data rate maximization.

A. Problem Formalization

We consider the system that contains a set of N_{UE} UEs, $\mathcal{N}_{\text{UE}} = \{1, ..., N_{\text{UE}}\}$. We also assume a set of candidate sites for the RIS placement, $\mathcal{L}_{\text{RIS}} = \{1, ..., L_{\text{RIS}}\}$, where L_{RIS} is the number of possible RISs' locations. Similarly, a set of BSs' locations is defined as $\mathcal{L}_{\text{BS}} = \{1, ..., L_{\text{BS}}\}$ with L_{BS} being the number of possible BSs' locations. The data rate of UE i associated with the RIS and the BS located at nodes j and k, D_{ijk}, is calculated as per (12).

To model the optimization problem of optimal RIS deployment, we denote the UE-RIS-BS association variable, u_{ijk}, as a binary indicator. Let $u_{ijk} = 1$ if UE i is associated with the RIS located at node j and BS located at node k, and $u_{ijk} = 0$ otherwise. Moreover, we introduce a binary indicator, x_j, to specify the RIS location variable, i.e., $x_j = 1$ if a RIS is placed at node j, and $x_j = 0$ otherwise. In this case, node j represents one of the possible sites for RIS placement.

We then assume that UE i can be associated with node j, only if RIS j is activated:

$$u_{ijk} \leq x_j, i \in \mathcal{N}_{\text{UE}}, j \in \mathcal{L}_{\text{RIS}}, k \in \mathcal{L}_{\text{BS}}. \tag{13}$$

Similarly, we assume that UE i can be associated with BS k, only if BS k is activated. Hence, we introduce a binary indicator, y_k, to denote the BS location variable. Let $y_k = 1$ if a BS is placed at node k, and $y_k = 0$ otherwise.

$$u_{ijk} \leq y_k, i \in \mathcal{N}_{\text{UE}}, j \in \mathcal{L}_{\text{RIS}}, k \in \mathcal{L}_{\text{BS}}. \tag{14}$$

Moreover, we impose a limit to the number of RISs and BSs to be deployed:

$$1 \leq \sum_{j \in \mathcal{L}_{\text{RIS}}} x_j \leq N_{RIS}, \tag{15a}$$

$$1 \leq \sum_{k \in \mathcal{L}_{\text{BS}}} y_k \leq N_{\text{BS}}, \tag{15b}$$

where N_{RIS} and N_{BS} are the maximum number of employable RISs and BSs, respectively. Then, the optimal multi-RIS deployment in 5G NR/6G cellular networks with directional antennas takes the following form:

$$\max \sum_{i \in \mathcal{N}_{\text{UE}}} \sum_{j \in \mathcal{L}_{\text{RIS}}} \sum_{k \in \mathcal{L}_{\text{BS}}} D_{ijk} u_{ijk}. \tag{16}$$
$$\text{s.t. } (13), (14), (15).$$

However, unlike RIS deployment, which is still an ongoing activity, BS deployment is already fixed. Therefore, the RIS placement problem with 1 predefined BS at location α might be considered. Hence, (15b) can be rewritten as:

$$y_{k=\alpha} = 1. \tag{17}$$

The pseudo-code in Algorithm 1 describes optimal solution according to (16). The algorithm employs our analytical

Algorithm 1: Optimal RIS Placement

Input: UEs coordinates, N_{RIS}, N_{BS}, $\mathcal{L}_{\text{RIS}}$, $\mathcal{L}_{\text{BS}}$;
Output: Optimal solution for RIS placement;
Calculate blockage probability p_{B} as per (3);
Calculate LoS probability p_{L} as per (4);
Extract the channel condition of each UE;
Solve the problem (16).

framework to find the optimal placement of one or more RISs among different possible locations to maximize the total data rate. Note that we solve the problem using *branch and bound algorithm* by employing a series of techniques (e.g., size reduction and linear programming relaxation, among others) to enhance the algorithm's efficiency. The branch-and-bound algorithm decomposes the original problem into sub-problems, which provide an upper and lower bound on the solution. Some of them can improve the current upper and lower bound. Initially, the upper bound is any feasible solution, and the lower bound is the relaxed problem solution. The algorithm stops when the difference between upper and lower bounds is less than a predefined value or the spent time/number of iterations surpasses the threshold.

The optimal multi-RIS deployment in 5G NR/6G networks with directional antennas is NP-hard since it represents a facility location problem that is proven to be NP-hard [17].

IV. Selected Numerical Results

This section collects the main numerical results on optimal RIS deployment in 5G NR/6G obtained using the proposed optimization framework. First, we analyze the optimal deployment of a single RIS to study the impact of RIS height (i.e., the relationship between heights of a BS and a RIS) on the system performance. Then, we investigate the effect of blocker density and the number of UEs for a single-RIS system. Finally, the impact of UE distribution on multiple RISs deployments is examined, and the optimal RISs placement is shown. The transmission parameters for simulations are set up as indicated in Table I and below.

TABLE I
Default parameters for numerical assessment.

Parameter	Value
Number of UEs, N_{UE}	30
Blockers density, λ_{B}	20%
Probability of no-connection, $P_{\text{no-connection}}$	20%
Number of possible RIS locations, L_{RIS}	220
Service area width, h_{SA}	100 m
Service area length, b_{SA}	50 m
UE distribution	Uniform/Matérn cluster pr.
Number of clusters	5
Operating frequency, f_c	28 GHz
Bandwidth, W_{GHz}	1 GHz
Power Spectral Density of Noise, N_0	$10^{-\frac{174}{10}}$ W/Hz
Antenna Transmit Power, P_t	0.2 W
Receiver Antenna Gain, G_{rx}	3.6058 (linear scale)
Transmitter Antenna Gain, G_{tx}	28.7078 (linear scale)
Number of Reflective Elements, NN	2048
Reflective Element Gain, Γ	1
BS height, h_{BS} / RIS height, h_{RIS}	10 m
UE height, h_{UE}	1.5 m
Blocker radius, r_{B}	0.4 m
Blocker height, h_{B}	1.7 m
Number of BS, N_{BS}	1
Number of employable RISs, N_{RIS}	1-10

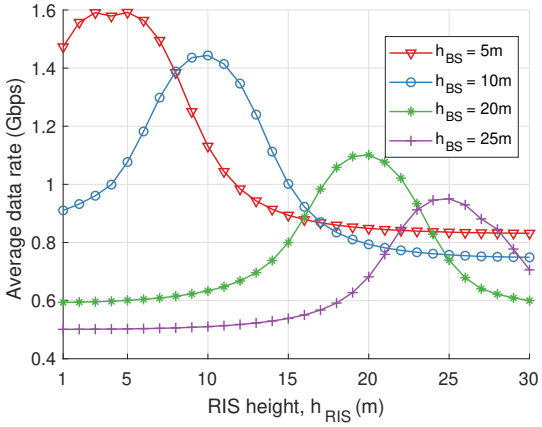

Fig. 2. Average data rate as function of RIS height, single RIS.

We assume that UEs in LoS non-blocked conditions communicate directly with the BS. We also suppose that some UEs cannot use the RIS to reach the BS (with no-connection probability[1] of 0.2 by default). Hence, these UEs are forced to communicate directly with the BS, independently of their channel conditions. For RIS placement, we consider a grid of possible locations [18]. That is, a RIS can be placed only in one of the defined sites. Note that using a set of possible locations reduces problem complexity without weakening the validity of our solution. Moreover, it is not feasible to locate a RIS in any place in a real-case scenario due to geographical and bureaucratic constraints. Further, we suppose that a RIS is in LoS conditions with the BS and the UEs [16], whereas NLoS conditions to/from RISs are taken into account through no-connection probability. The BS is deployed at the center of the area of interest.

Furthermore, we implement four benchmarks to analyze the performance of RIS-aided communication:

- **LoS non-blocked, no RIS**. All UEs in the network are in LoS non-blocked conditions with the BS.
- **NLoS blocked, no RIS**. All UEs in the network are in NLoS blocked conditions with the BS.
- **Mixed scenario, no RIS**. The UEs in the network have different channel conditions with the BS (see Section II).
- **Random RIS deployment**. UEs in the network are associated with a randomly deployed RIS.

We first investigate the impact of RIS height on the average data rate for optimal RIS placement with 2048 reflective

[1]The probability that a UE cannot use a RIS to enhance performance. The inability to communicate with the RIS can be caused by different reasons, such as NLoS condition between the UE and the RIS.

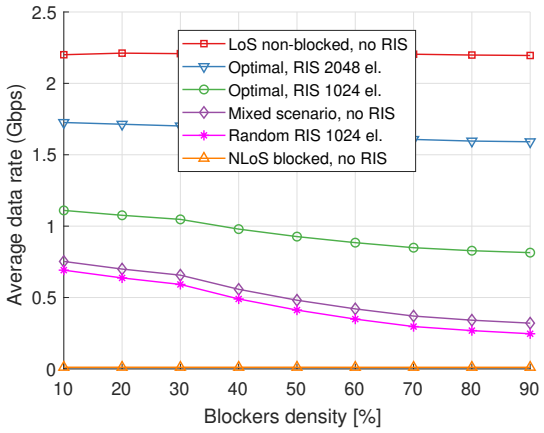

Fig. 3. Average data rate as function of blocker density, single RIS.

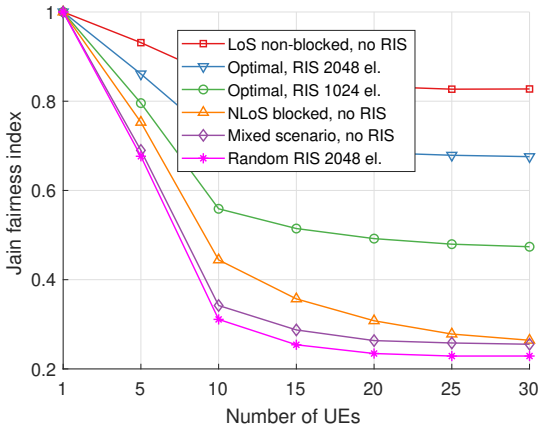

Fig. 4. Jain fairness index as function of number of UEs, single RIS.

elements, as shown in Fig. 2. In this scenario, we consider uniform UE distribution, and the optimal RIS placement obtained through the proposed framework is near the BS. We observe that the peak of each curve (except for $h_{\text{BS}} = 5\,\text{m}$) is reached when RIS height, h_{RIS}, is equal to BS height, h_{BS}. The rationale is that the BS-RIS distance is minimized when h_{RIS} and h_{BS} are the same for the given simulation layout (when RIS is optimally placed near the BS). For example, we refer to dashed links from the NR BS to any RIS in Fig. 1. Geometrically, this distance is smaller if both NR BS and RIS are of equal height. Differently, in the case of $h_{\text{BS}} = 5\,\text{m}$ (see triangles in Fig. 2), one can notice two peaks at $h_{\text{RIS}} = 3\,\text{m}$ and $h_{\text{RIS}} = 5\,\text{m}$. We emphasize that the peak at 5 m slightly outnumbers the one at 3 m and explain this behavior by the low heights of BS and RIS. Moreover, at given blocker density of $\lambda_B = 0.2$, one can see that a lower BS height allows for achieving a higher average data rate since both the RIS and the BS are closer to the UEs (i.e., the second dashed link from RIS to UE in Fig. 1 is smaller when the RIS is placed closer to the UE in terms of its height). However, low RIS height might cause a higher blockage probability under a higher blocker density scenario compared to higher RIS.

By varying the blocker density (see Fig. 3), we can quantify the impact of RIS usage on the system performance. We can see that, as expected, the average data rate decreases as the blocker density increases in both scenarios with and without RIS-enhanced communications. The reason is that a higher blocker density, λ_{B}, implies a higher probability that UEs' communication paths are blocked by pedestrians, leading to channel conditions deterioration. Moreover, Fig. 3 shows the importance of optimal RIS placement since a random placement yields worse results than the scenario without RIS. Hence, poorly placed RIS worsens the performance instead of improving it. LoS non-blocked and NLoS blocked scenarios are not influenced by blockers density by default.

We now consider the Jain fairness index to analyze the system performance, as shown in Fig. 4. Fairness determines whether UEs are receiving a fair share of network resources. A fair system has a value of 1, whereas a fully unfair system maintains 0. We can learn that RIS-aided scenarios outperform Mixed and NLoS blocked ones in a multiple user configuration[2], demonstrating that a properly placed RIS enhances the performance of poor-quality links. We also note that RISs can limit the fairness worsening among UEs only under optimal placement since a random RIS deployment leads to the unfairest system. We emphasize that in the case of a single-UE single-RIS scenario, an optimal RIS placement strategy is either near the BS or the UE. In contrast, an optimal RIS deployment is near the BS in the case of single RIS and multiple uniformly distributed UEs. These solutions guarantee a reduction in the total path loss experienced by the UEs.

Finally, we analyze the impact of UE distribution and RIS height on the deployment of 10 RISs. Specifically, we examine uniform UE distribution and UE distribution according to Matérn cluster process with 5 clusters containing 6 UEs each, for $h_{\text{RIS}} = 5\,\text{m}$ and $h_{\text{RIS}} = 10\,\text{m}$ RIS heights. We note that the two RISs out of ten are placed near the BS, both in case of uniform and clustered UE distribution, if $h_{\text{RIS}} = 10\,\text{m}$ (see Fig. 5(a) and Fig. 5(c)). Conversely, UE distribution greatly impacts RIS deployment when $h_{RIS} = 5\,\text{m}$. Namely, in the case of uniform UE distribution, 1 RIS is placed near the BS, and the remaining 9 RISs next to a UE (see Fig. 5(b)). In the case of cluster UE distribution, 5 RISs out of 10 are deployed each next to a cluster of UEs, while the remaining ones are not utilized (see Fig. 5(d)). The performance of the examined scenarios in terms of average data rate and average latency [3] is reported in Table II.

V. Conclusion

To reduce the impact of human blockage and NLoS links, upcoming 5G NR/6G cellular networks are expected to employ RIS to achieve LoS-dominated channels. However, the RIS deployment strategy has still to be fully explored to allow RIS employment in real-world scenarios. In this work, we have

[2]Multiple users communicate separately with the BS.

[3]To transmit one frame of 8K, 8 bit with 150 compression rate.

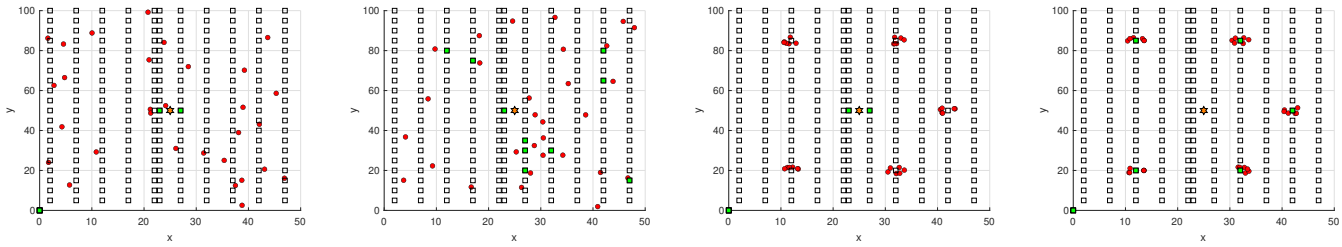

(a) (b) (c) (d)

Fig. 5. Multi-RIS topology (red circles represent UEs, white squares - possible RIS sites, green squares - optimal RIS sites, orange hexagram is the BS): (a) Uniform, $h_{\text{RIS}} = 10\,\text{m}$, (b) Uniform, $h_{\text{RIS}} = 5\,\text{m}$, (c) Clusters, $h_{\text{RIS}} = 10\,\text{m}$, and (d) Clusters, $h_{\text{RIS}} = 5\,\text{m}$.

TABLE II
ANALYSED TOPOLOGIES, MULTI-RIS CASE, $h_{\text{BS}} = 10\,\text{M}$.

Layout	**Average data rate**	**Average latency**	**Specifics (close to)**
Uniform, $h_{\text{RIS}} = 10\,\text{m}$	1.7721 Gbps	2.6628 ms	BS
Uniform, $h_{\text{RIS}} = 5\,\text{m}$	1.0876 Gbps	4.3386 ms	BS and UEs
Hotspot, $h_{\text{RIS}} = 10\,\text{m}$	1.4907 Gbps	3.1654 ms	BS
Hotspot, $h_{\text{RIS}} = 5\,\text{m}$	0.8259 Gbps	5.7134 ms	hotspots

formulated the RIS deployment problem in 5G NR/6G cellular networks with directional antennas as a facility location problem that maximizes the total data rate. Moreover, we have evaluated and analyzed the impact of various parameters on RIS-aided communication performance, such as RIS height, blocker density, and number of UEs. Our numerical results showed the positive impact of RIS over poor-quality links and system performance when the RIS is deployed near the BS in a single-BS single-RIS system. Moreover, we analyzed UE distribution impact on the deployment of multiple RISs, showing that a variation in RIS height and/or in UE distribution resulted in different RISs deployment strategies.

This study may serve as a tool for optimizing and analyzing RIS deployment in different scenarios. As a future research direction, one may design a low-complexity heuristic or implement machine learning algorithms to reduce complexity at the expense of accuracy while striking the complexity-performance balance. Further, regarding the scenario with dynamic users, one may analyze the most common user distribution in the particular area to decide where to deploy RISs and how many.

ACKNOWLEDGMENT

The authors gratefully acknowledge funding from European Union's Horizon 2020 Research and Innovation programme under the Marie Skłodowska Curie grant agreement No. 813278 (A-WEAR, http://www.a-wear.eu/).

REFERENCES

[1] W. Jiang, B. Han, M. A. Habibi, and H. D. Schotten, "The Road Towards 6G: A Comprehensive Survey," *IEEE Open Journal of the Communications Society*, vol. 2, pp. 334–366, 2021.

[2] C. Pan, H. Ren, K. Wang, J. F. Kolb, M. Elkashlan, M. Chen, M. Di Renzo, *et al.*, "Reconfigurable Intelligent Surfaces for 6G Systems: Principles, Applications, and Research Directions," *IEEE Communications Magazine*, vol. 59, no. 6, pp. 14–20, 2021.

[3] Q. Wu, S. Zhang, B. Zheng, C. You, and R. Zhang, "Intelligent Reflecting Surface Aided Wireless Communications: A tutorial," *IEEE Transactions on Communications*, 2021.

[4] S. Zhang and R. Zhang, "Intelligent Reflecting Surface Aided Multiple Access: Capacity Region and Deployment Strategy," in *2020 IEEE 21st International Workshop on Signal Processing Advances in Wireless Communications (SPAWC)*, pp. 1–5, IEEE, 2020.

[5] S. Zhang and R. Zhang, "Intelligent Reflecting Surface Aided Multi-User Communication: Capacity Region and Deployment Strategy," *IEEE Transactions on Communications*, vol. 69, no. 9, pp. 5790–5806, 2021.

[6] Y. Zhang, J. Zhang, M. Di Renzo, H. Xiao, and B. Ai, "Reconfigurable intelligent surfaces with outdated channel state information: centralized vs. distributed deployments," *IEEE Trans. on Communications*, 2022.

[7] Y. Li, C. Yin, T. Do-Duy, A. Masaracchia, and T. Q. Duong, "Aerial Reconfigurable Intelligent Surface-Enabled URLLC UAV Systems," *IEEE Access*, vol. 9, pp. 140248–140257, 2021.

[8] Q. Bie, Y. Liu, Y. Wang, X. Zhao, and X. Y. Zhang, "Deployment Optimization of Reconfigurable Intelligent Surface for Relay Systems," *IEEE Transactions on Green Communications and Networking*, vol. 6, no. 1, pp. 221–233, 2022.

[9] O. Chukhno, N. Chukhno, O. Galinina, S. Andreev, Y. Gaidamaka, K. Samouylov, and G. Araniti, "A Holistic Assessment of Directional Deafness in mmWave-based Distributed 3D Networks," *IEEE Transactions on Wireless Communications (Early Access)*, 2022.

[10] 3GPP, "Study on Channel Model for Frequencies from 0.5 to 100 GHz (Release 14)," 3GPP TR 38.901 V14.1.1, July 2017.

[11] M. Gapeyenko, V. Petrov, D. Moltchanov, M. R. Akdeniz, S. Andreev, N. Himayat, and Y. Koucheryavy, "On the Degree of Multi-Connectivity in 5G Millimeter-wave Cellular Urban Deployments," *IEEE Transactions on Vehicular Technology*, vol. 68, no. 2, pp. 1973–1978, 2018.

[12] M. Gapeyenko, A. Samuylov, M. Gerasimenko, D. Moltchanov, S. Singh, E. Aryafar, S.-p. Yeh, N. Himayat, S. Andreev, and Y. Koucheryavy, "Analysis of Human-Body Blockage in Urban Millimeter-Wave Cellular Communications," in *2016 IEEE International Conference on Communications (ICC)*, pp. 1–7, IEEE, 2016.

[13] X. Tian, N. Gonzalez-Prelcic, and R. W. Heath Jr, "Optimizing the Deployment of Reconfigurable Intelligent Surfaces in MmWave Vehicular Systems," *arXiv preprint arXiv:2205.15520*, 2022.

[14] S. Zeng, H. Zhang, B. Di, Z. Han, and L. Song, "Reconfigurable Intelligent Surface (RIS) Assisted Wireless Coverage Extension: RIS Orientation and Location Optimization," *IEEE Communications Letters*, vol. 25, no. 1, pp. 269–273, 2020.

[15] S. W. Ellingson, "Path loss in Reconfigurable Intelligent Surface-enabled Channels," in *2021 IEEE 32nd Annual International Symposium on Personal, Indoor and Mobile Radio Communications (PIMRC)*, pp. 829–835, IEEE, 2021.

[16] I. Yildirim, A. Uyrus, and E. Basar, "Modeling and Analysis of Reconfigurable Intelligent Surfaces for Indoor and Outdoor Applications in Future Wireless Networks," *IEEE Transactions on Communications*, vol. 69, no. 2, pp. 1290–1301, 2020.

[17] H. A. Eiselt and V. Marianov, *Foundations of location analysis*, vol. 155. Springer Science & Business Media, 2011.

[18] M. Unbehaun and M. Kamenetsky, "On the Deployment of Picocellular Wireless Infrastructure," *IEEE Wireless communications*, vol. 10, no. 6, pp. 70–80, 2003.